Expression of γδTCR on myeloid cells of Plasmodium yoelii nigeriensis -infected C57BL/6 mice

Dianhui Chen
the Third Affiliated Hospital of Guangzhou Medical University
Feng Mo
the Third Affiliated Hospital of Guangzhou Medical University
Meiling Liu
The Third Affiliated Hospital of Guangzhou Medical University
Lin Liu
China Sino-French Hoffmann Institute, Guangzhou Medical University
Junmin Xing
China Sino-French Hoffmann Institute, Guangzhou Medical University
Feihu Shi
the Third Affiliated Hospital of Guangzhou Medical University
Anqi Xie
China Sino-French Hoffmann Institute, Guangzhou Medical University
Hongyan Xie
China Sino-French Hoffmann Institute, Guangzhou Medical University
Xingfei Pan
the Third Affiliated Hospital of Guangzhou Medical University
Xinhua Wang
The First Affiliated Hospital of Guangzhou Medical University
Jun Huang (hj165@sina.com)
China Sino-French Hoffmann Institute, Guangzhou Medical University

Research Article

Keywords: Plasmodium yoelii nigeriensis , γδTCR+CD11b+ cells, pathways

Posted Date: April 18th, 2022

DOI: https://doi.org/10.21203/rs.3.rs-1552209/v1

Abstract

Background: The role of $CD3^+\gamma\delta TCR^+$(γδT) cells during the *Plasmodium yoelii nigeriensis* infection has been reported in our previous studies. However, there is a paucity of studies on the characteristics of myeloid cells which expressed γδTCR. Therefore, the aim of this study was to observe the properties of γδTCR-expressing myeloid cells in the spleen of C57BL/6 mice infected by *P. yoelii NSM.*

Methods: Haematoxylin-eosin (HE) staining was used to observe the pathological changes in the spleens. The samples from the experimental group before and after infection underwent RNA sequencing (RNA-seq), and the differentially expressed genes (DEGs) were screened. Flow cytometry (FCM) was used to evaluate the frequency of $\gamma\delta TCR^+$ cells and the characteristics of $\gamma\delta TCR^+$ cells in *Plasmodium yoelii*-infected mice.

Results: We observed obvious infiltration of inflammatory in infected C57BL/6 mouse spleens. The proportions of $\gamma\delta TCR^+$ cells and $CD11b^+$ $\gamma\delta TCR^+$cells from infected group were higher than that from normal group. $\gamma\delta TCR^+CD11b^+$ cells expressed high levels of activated-mediated genes and inflammatory-mediated genes. We characterized the heterogeneous pathway activities among $\gamma\delta TCR^+CD11b^+$ cells from normal and infected group. The oxidative phosphorylation, respiratory electron transport chain and leukocyte activation involved in immune response pathways were up-regulated, while the alpha-beta T cell activation and myeloid leukocyte migration pathways were down-regulated. Importantly, we found that *Ly6c2* was higher expressed in $\gamma\delta TCR^+CD11b^+$ cells than *Ly6g*. Consistent with it, flow cytometry results revealed that a subset of $Ly6C^+Ly6G^-CD11b^+\gamma\delta TCR^+$ cells was higher than $Ly6G^+Ly6C^-CD11b^+\gamma\delta TCR^+$ cells in the spleen.

Conclusions: Taken together, our data suggest the existence of a population of γδTCR-expressing myeloid cells and played potential role in the context of *Plasmodium* infection. The molecular markers and pathways screened warrant further study.

Introduction

Malaria is a mosquito-borne infectious disease of humans and animals caused

by parasitic protozoans of the genus *Plasmodium*[1]. Malaria remains one of the most

lethal infectious diseases worldwide due to the increased resistance to artemisinin and

limited vaccine efficacy[2, 3]. The human disease is caused by five different parasitic species, with *Plasmodium falciparum* being the deadliest[4]. *P. yoelii nigeriensis* NSM is a subspecies of the rodent malaria parasite that become pivotal model systems for understanding the malaria pathogenesis[5, 6].

The immune system is fundamentally divided into the innate and adaptive arms, predominantly represented by the myeloid and lymphoid lineages[7]. The three major groups of myeloid cells are

essential to the proper functioning of both our innate and adaptive immune systems: macrophagess, dendritic cells, and granulocyte[8]. The studies revealed that monocytes and macrophages play crucial roles in parasite clearance, especially in immunologically naïve individuals lacking malaria-specific antibodies, though they also participate in the pathological events[9, 10]. Further evidence demonstrates that Dendritic cells (DCs) are crucial for the initiation of effective immune responses, including cellular and antibody responses to *P. falciparum*[11, 12]. In addition, the neutrophils, which are most populous in the circulation; and several other granulocyte subsets, such as eosinophils, basophils, and mast cells, which also expand rapidly in either the blood stream or tissues during particular parasite infections[7].

Gamma delta T cells, the first line of immune response against invading pathogens, display a number of effective functions leading to cells proliferation, release of pro- and anti-inflammatory cytokines, and also cytotoxic molecules(eg. granzyme A, B)[13, 14]. The studies of human and murine malaria demonstrate γδT cells are expanded with different strains of *Plasmodium.* Further evidence demonstrates that the γδ T cell compartment plays a role in the post-acute stage of the infection[15]. The longstanding tenet that TCR expression is a prerequisite of T lymphoid cells was approved. However, the presence of TCR-based immunoreceptors in the granulocyte lineage is supported by Legrand's study which revealed the presence of a functional TCRγδ in human eosinophil granulocytes[16]. Consistent with this concept, a previous study from our laboratories provides evidence that a subpopulation of $CD3^{-}$γδ TCR^{+} cells was found in the liver, which play potential roles within site of *S. japonicum* infection in C57BL/6 mouse liver [14]. The presence of these TCR-like receptors is not limited to peripheral blood monocytes and T-lymphocytes, but they may be also found in tissue myeloid cells at sites of inflammation.

Hence, this study will primarily focus on the phenotype and function of expression of γδTCR on myeloid cells and the potential important mechanisms that affect the *Plasmodium yoelii* progression.

Materials And Methods

Mice

Female C57BL/6(6-8 week old) mice were purchased from Traditional Chinese Medicine University of Guangzhou Animal Center (Guangzhou, China). All animal experiments were performed in strict accordance with the Regulations for the Administration of Affairs Concerning Experimental Animals (1988.11.1). The animal protocols were approved to be appropriate and humane by the institutional animal care and use committee of Guangzhou Medical University (2012-11).

Infection

Plasmodium yoelii nigeriensis NSM was purchased from the malaria research and reference reagent resource center (MR4). Frozen *P. yoelii* were thawed and injected into C57BL/6 mice. The blood was collected when the parasitaemia up to 10%-15% after 2-3 days. C57BL/6 mice (6–8 weeks, female) were infected with 1×10^{6} infected red blood cells. Then they were euthanized 12 days after infection. Pathogen-free C57BL/6 mice were used as controls.

Antibodies

APC-cy7-conjugated anti-mouse CD3 (145-2C11), FITC-conjugated anti-mouse CD3 (17A2), FITC-conjugated anti-mouse γδ TCR (B1), BV510-conjugated anti-mouse γδ TCR (GL3), PE-Cy5-conjugated anti-mouse (6D5), PE-cy7-conjugated anti-mouse CD11b(M1/7), PerCPCy5.5-conjugated anti-mouse Ly-6C(HK1.4), PE-conjugated anti-mouse Ly6G (1A8) were purchased from BioLegend (San Diego, CA, USA) and BD Pharmingen (San Diego, CA, USA).

Histology Studies

Spleens were removed from mice, perfused with 0.01 M phosphate-buffered saline (pH = 7.4) for three times, fixed in 10% formalin, embedded in paraffin, and serially sectioned. Standard hematoxylin and eosin (H&E) staining for visualization of cellular changes under microscopy (Olympus ix71) was done.

10x Genomics Chromium library construction and sequencing

12 days after *P. yoelii* NSM infection, mice were sacrificed and spleens were collected from three infected and three naive mice, mixed respectively. Cells were collected, and the expression of RNA in each cell were detected by 10× Genomics Chromium Single Cell RNA Sequencing (LC-biotechnology, LTD, Hangzhou, China). GemCode^{TM} Single Cell platform (10X Genomics, Pleasanton, CA) was used to determine the transcriptomes of single cells. 15 μl of single-cell suspension at a concentration of ~900,000 cells/ml was loaded into one channel of the ChromiumTM Single Cell G Chip (10X Genomics, 1000073), aiming for a recovery of 8000-9000 cells. The Chromium Single Cell 3'Library & Gel Bead Kit v3 (10X Genomics, 1000075) was used for single-cell barcoding, cDNA synthesis and library preparation, following manufacturer's instructions according to the Single Cell 3'Reagent Kits User Guide Version 3. Libraries were sequenced on Illumina Novaseq6000 using paired-end 150 bp.

scRNA-seq data processing, quality control and filtering

We used CellRanger(version 5.0.1), aligned reads on the GRCm38 reference genome for mouse and generated unique molecular identifier gene expression profiles for every single cell under standard sequencing quality threshold (default parameters). Low-quality cells were removed for downstream analysis when they met the following criteria for retaining cells: (1) ≥50,000 sequence reads; (2) ≥40% of reads uniquely aligned to the genome; (3) ≥40% of these reads mapping to RefSeq annotated exons.

Through Seurat (Version 4.1.0) R package, we processed the UMI counts mentioned above with further filteration criteria(cells are removed): 1) less than 200 and more than 6000 expressed genes, 2) higher than 10% mitochondrial genome transcript, 3) Genes expressed in less than 3 cells, 4) more than 50000 UMI counts. Eventually, 28846 cells and 17730 genes were kept in data.

Normalization, Scaling and clustering

We normalized the final filtered gene expression data matrix using “NormalizeData” function with default setting. We choose 3000 highly variable genes via “FindVariableGenes” function from the final filtered count matrix and then centered and scaled them via “ScaleData” function. We then performed principle component analysis (PCA) on the 3000 genes by “RunPCA” function. The dimensional reduction were performed through Canonical correlation analysis (CCA) in Seurat. Cells were clustered by “FindClusters” function and the clustered cells were then projected onto a two-dimensional space using “RunT-SNE” function. The clustering results were visualized by “DimPlot” function.

Identification of DEGs and enrichment analysis

Differentially expressed genes (DEGs) were identified by “FindMarkers” function in Seurat using “wilcox” test methods and Bonferroni correction. Significant DEGs were selected from genes with adjusted P value(p_val_adj) ≤ 0.05 and log processed average fold change(avg_log2FC) ≥ 0.25 for further analysis and visualization. GO analysis and KEGG pathway enrichment analysis of these significant DEGs were performed by clusterProfiler package.

$CD11b^{+}Tcrg\text{-}C2^{+}$ cells in normal(YX484) and 12dpi(YX391) groups were used to perform differentially expressed analysis, and genes with p Value < 0.05 were selected for further GO/KEGG annotation and enrichment via clusterProfiler R package (v 4.0.5).

Lymphocyte Isolation

Mice were euthanized at12 days after infection. Mice were perfused with sterile saline to remove blood from the body before obtaining the spleen tissue. The excised spleen was pressed through a 200-gauge stainless-steel mesh and suspended in Hank’s balanced salt solution. Mouse Lymphocyte Separation Medium (DAKEWE, China) density gradient centrifugation was used to isolate lymphocytes. The isolated cells were washed in HBSS and re-suspended at 2×10^{6} cells/ml in complete RPMI 1640 medium, which were prepared for flow cytometry analysis.

Cell Surface Staining

Cells were washed in PBS and blocked in PBS buffer containing 1% BSA for 30min. Cells were then stained with conjugated antibodies specific for the cell surface antigens for 30min at 4◦C in the dark. Expressions phenotypes of antibody-labeled cells were analyzed by flow cytometry (Beckman CytoFLEX), and the results were analyzed using the CytExpert 1.1 (Beckman Coulter Inc.). Isotype-matched controls for cell surface markers were included in each staining protocol.

Statistics

Data were analyzed by SPSS 21.0 and statistical evaluation of the difference between means was assessed using one-way ANOVA. $P < 0.05$ was considered to be statistically significant.

Result

Pathological changes of the spleen of the infected mice

To examine the pathological changes in the spleens of *Plasmodium yoelii*-infected mice, the mice were euthanized 12 days post-infection and the spleens were removed. As shown in Fig. 1A, the size and colour of the spleens in the infected group is bigger and darker compared with the normal control group. The weight of the spleen and the number of spleen cells from infected mice were significant higher than that from the normal control mice (***P<0.001,**P<0.01). Paraffin sections were made and stained with hematoxylin and eosin to observe the effects of infection on spleen microstructure. Splenic sinusoid hyperemia, germinal center hyperplasia and cellular infiltration of T cells were noted in the spleen of the infected mice(Fig. 1D).

The induced γδTCR$^+$ cells and CD11b$^+$γδTCR$^+$ cells in the spleen of the infected mice

In order to examine the role of γδTCR$^+$ cells, we compared scRNA-seq data from normal control spleen cells, to infected cells. After filtering cells, a total of 11656 cells in normal spleen and 9998 cells in infected spleen remained for analysis. After UMAP projection of cell clusters, there was a total of 12 distinct clusters representing major spleen groups. Feature plots showing the expression of *Tcrg-C2* gene was cell-type specific, with predominance for expression in CD4$^+$T cell and CD8$^+$T cell from normal group (Fig. 2A). In contrast, *Tcrg-C2* gene was mainly enriched in NKT cells/ γδT cells after infection. The frequency of cells expressing *Tcrg-C2* among all cells from infected group was higher than normal control group. We observed the expression of CD3, CD19, as well as CD11b in *Tcrg-C2*-expressing cells (Fig. 2C). It is clear that the infected group has a much greater proportion of CD11b-expressing cells amongst *Tcrg-C2*-expressing cells than is the case with normal group. We then explored the expression γδTCR$^+$CD3$^+$ cells, γδTCR$^+$CD19$^+$ cells, γδTCR$^+$CD11b$^+$ cells by incubating with different fuorescence labeled markers. The γδTCR$^+$cells were gated first, and then expression levels of CD3, CD19 and CD11b were examined by FACS (Fig. 2D). The proportions of γδTCR$^+$ cells and γδTCR$^+$ CD3$^+$cells were higher (P < 0.05) compared with that in the normal mice. There was no obvious different in the γδTCR$^+$CD3$^+$ cells and γδTCR$^+$CD19$^+$ cells between the normal and infected hosts.

The differentially expressed genes (DEGs) analysis

Regarding the large amount of data obtained by RNAseq, we conducted a screen of the genes in 12dpi *vs.* control groups and obtained 4759 genes for further analysis. We utilized the ballgown package of R to analyze the DEGs of the String Tie-assembled and-quantified genes (P<0.05 or Q<0.05), and the differential expression multiple was screened as >1.5. Then, we obtained 330 DEGs: 212 were up-regulated and 118 were down-regulated (Fig. 3), where *Gzmb, Gzma, Ccl5, Ccl4* and *Ccl3* were significantly up-regulated and *Il1b, Ccr7* and *Il7r* were significantly down-regulated.

The state of the Splenetic γδTCR$^+$CD11b$^+$cells

The states of the infected *Itgam* and *Tcrg-C2* co-expressing cells (γδTCR$^+$CD11b$^+$ cells) were determined by measuring the *Klrk1, Klrc1, Sell, Cd44, Cd69, Il2ra, Fcgr3, Cd40, Pdcd1, Cd274, Btla*, and *Havcr2* gene expressions. Violin plots showed expression level of genes. The black whiskers extended from the bars represent the upper (max) and lower (min) adjacent values in the data. The black lines in the middle of the bars showed the median values (Fig. 4A). *Klrc1* (NKG2A), *Cd40* (CD40), *Pdcd 1*(PD-1), *Havcr2* (CTLA-4) highly expressed in infected γδTCR$^+$CD11b$^+$ cells compared to normal cells. Comparing to normal γδTCR$^+$CD11b$^+$ cells, infected cells expressed lower levels of *Klrk1, Sell, Cd274, Btla* genes, which was validated by single-cell RNA sequencing. Similar phenomenon was observed in results of proportion of cells that expressed those genes within the whole γδTCR$^+$CD11b$^+$ population(Fig. 4B).

Cytokine Gene Expressions of γδTCR$^+$ CD11b$^+$Cells

Since the cytokine–cytokine receptor interaction was enriched in γδTCR$^+$CD11b$^+$ cells, we investigated the expression level of cytokine expression profiles in γδTCR$^+$ CD11b$^+$ cells. Although many cytokine genes are known to be involved in the infection, we filtered for some differentially expressed genes in two groups(Fig. 5). Notably, violin plots confirmed that *Ifng, Il10, Fas* and *Csf1* were highly expressed in infected groups and the expressions of *Il1b* and *Tnf* were decreased. In line with the above findings, the proportion of cells that expressed those genes within the whole γδTCR$^+$CD11b$^+$ population showed the same trend (Fig. 5B).

The functional analyses of DEGs

After identifying DEGs, we analyzed the DEGs using Gene Ontology enrichment analysis to explore the potential functions of these genes. The up-regulated genes and down-regulated genes in the 12dpi *vs.* control cells were evaluated by GO analysis, respectively(Fig. 6). In comparison with the normal cells, the infected cells expressed high levels of genes were enriched in the items related to energy metabolism, including oxidative phosphorylation and respiratory electron transport chain. It revealed that in addition to the items related to energy metabolism, infammatory-related pathways, especially leukocyte activation involved in immune response, was also enriched among the up-regulated DEGs (Fig. 6B). The genes, including *Ndufs8, Cox5b, Uqcrb, Lgals1, Pycard,* and *Ifng*, were highly expressed in the 12dpi *vs.* control cells. Moreover, down-regulated genes related, such as *Ccr7, Itch, Foxp1, Tcf7* and *Cd44*, were mainly enriched in alpha-beta T cell activation pathway. The analysis of the down-regulated genes showed that the functions of a series of genes were also related to myeloid leukocyte migration, such as *Dusp1*, *Il1b, Ccr7, Fcer1g* and *Il17ra*(Fig. 6D).

Phenotypic Changes in Splenetic γδTCR$^+$ CD11b$^+$ Cells

To study the characteristics of γδTCR$^+$ CD11b$^+$ cells during *Plasmodium yoelii*

infection, the expressions of *Ly6*g and *Ly6c2* genes were detected. The scRNA-seq analysis showed that the γδTCR$^+$ CD11b$^+$ cells marked by high levels of *Ly6c2* in both infected and normal groups(Fig. 7A,B).

We then looked for evidence of different subsets expression γδTCR$^+$ CD11b$^+$ cells by incubating with different fuorescence labeled markers: Ly6G and Ly6C(Fig. 7C). The γδTCR$^+$CD11b$^+$ cells were gated first, and then expression levels of Ly6G and Ly6C were examined by FACS. The proportion of Ly6C$^+$ Ly6G$^-$ γδTCR$^+$ CD11b$^+$ cells was higher than that of Ly6G$^+$ Ly6C$^-$γδTCR$^+$ CD11b$^+$ cells in the normal and infected spleen (P<0.05). There was no obvious different in the Ly6C$^+$ Ly6G$^-$δTCR$^+$ CD11b$^+$ cells between the normal and infected hosts.

Discussion

The *Plasmodium*-infected red blood cells cause damage to organs through the blood circulatory system, including the spleen, liver, and so on. It initiates protective acquired immunity mediated mainly through CD4$^+$ T cells and antibody[17]. Macrophages or monocytes may also be involved in parasite control through releasing of parasiticidal mediators and in receptor-mediated phagocytosis [18]. Early responses in the spleen are vital factors modulating the clinical outcome of malaria infection[19]. The histopathological changes appear in the infected mouse spleen (Fig. 1) compared to uninfected controls showed that the spleen undergoes a series of morphological changes in response to *Plasmodium* infection. The most apparent is the enlargement of the spleen, including the weight and numbers of extracted spleen cells.

A significant expansion of populations of γδTCR$^+$ cells has been observed in the infected spleen compared with those control by scRNA-seq analysis and flow cytometry. The frequency of cells expressing *Tcr-C2* among all cells was increased during the infection, indicating that this population cells accumulated in the spleen and may play a role in the progress of *Plasmodium yoelii* infection (Fig. 2B). To further clarify the population of *Tcrg-C2*-expressing cells (γδTCR$^+$cells), the different subsets were examined, and differences between normal control and infected mice were compared. There was no obvious difference of the proportion of CD3$^+$T cells and CD19$^+$B amongst the *Tcrg-C2*-expressing cells from the infected and normal group. CD11b is usually expressed at high levels on macrophages and monocytes[20]. The higher frequency of CD11b-expressing cells amongst *Tcrg-C2*-expressing cells and a significant higher percentage of γδTCR$^+$CD11b$^+$cells in the infected spleen demonstrate the implication of CD11b$^+$γδTCR$^+$ cells at sites of inflammation, which might play a role during infection.

Furthermore, we investigated the activated state of γδTCR$^+$CD11b$^+$cells from stage of *Plasmodium*-infection in mice (Fig 4). The inhibitory (NKG2A) and activating (NKG2D and NKG2C) natural killer (NK) cell receptors are expressed on cytotoxic cells, all TCR γδT cells, and activated macrophages, which regulate the innate and adaptive immune systems related to cytotoxicity and cytokine production[21]. The γδT cells are subdivided into CD62L$^+$CD44$^-$ naïve cells, CD62L$^+$CD44$^+$ central memory cells (CM) and CD62L$^-$ CD44$^+$ effector memory cells (EM)[22]. PD-1, BTLA, and CTLA-4 are members of a family of inhibitory receptors that are responsible for various aspects of T-cell immune regulation including cell proliferation, cytokine production, and cytolytic activity[2, 23]. The results demonstrated that the *Plasmodium yoelii* infection facilitate activation of CD11b$^+$γδTCR$^+$cells and this population cells mediate

the immune response in the spleen of infected mice. Hence, the high expression of PD-1 and CTLA-4 may cause immunosuppression of antimalarial activity and restrict pathogens' clearance.

IFN-γ plays a role in controlling *Plasmodium* infection in both liver and blood stages of the parasite life cycle, but it can also exacerbate the severity of malarial disease depending on its temporal and spatial production[24]. IL-10 is an anti-inflammatory cytokine produced by many cell types, including T-helper type 2 cells, B cells, dendritic cells, macrophages, natural killer cells, eosinophils, and neutrophils[25]. Single-cell RNA sequencing of this expanded $CD11b^{+}\gamma\delta$ T CR^{+} cells population identified *CSf1*, which encodes M-CSF, a cytokine associated with myeloid cell recruitment and differentiation. M-CSF promotes survival and renewal

of monocytes and macrophages, and these cells represent an important frontline defense against *Plasmodium*[26]. The results showed that $CD11b^{+}\gamma\delta$ TCR^{+} cells are stimulated by Pf antigens and express high levels of IFN-γ, IL-10 and M-CSF, consistent with previous studies implicating myeloid cells up-regulated IL-10 during *Plasmodium chabaudi* infection in mice[17].

Compared with the normal sample, the infected sample was enriched for energy metabolism and leukocyte activation involved in immune response terms according to the GO results, and the bar graph results showed that associated genes, including that of *Ndufs8, Cox5b, Uqcrb, Lgals1, Pycard, Ifng*,and *Lgals1*, were upregulated. *Ndufs8* encode the protein complexes in mitochondrial inner membrane, which is participated in oxidative phosphorylation to cause mitochondrial dysfunction[27]. *Cox5b* is a growth-promoting gene that modulates downstream pathways in response to the induced bioenergetic alterations in breast cancer[28] and glioma[29], but its role in malaria remains unknown. These results further indicated that $CD11b^{+}\gamma\delta$ TCR^{+} cells might play an essential role in the progression of energy metabolism during the infection.

To further define this population of $CD11b^{+}\gamma\delta TCR^{+}$ cells, the different subsets were examined, and differences between normal control and infected mice were compared. Compared to Gr-1, Ly6C/Ly6G markers were better for identifying neutrophils, eosinophils, and both subsets of monocytes/macrophages in mouse[30]. Myeloid-derived suppressor cells (MDSCs) are subdivided into two major subsets: $Ly6G^{+}$ $Ly6C^{-}$granulocytic and $Ly6C^{+}Ly6G^{-}$ monocytic MDSCs[31], which can limit the ability to control infection through efficient anti-parasite immune responses[32] . The single-cell RNA sequencing and flow cytometry results showed that the $Ly6C^{+}Ly6G^{-}$ subset is the main subset in the infectious conditions. One study have characterized $CD11b^{high}Ly6C^{+}$cells that appear in the spleen of mice after an acute infection of *Plasmodium chabaudi* [17]. Our results were consistent with their results. Our findings revealed that they might be multifunctional cells, which play a role in all facets of immune responses, producing proinflammatory cytokines, inducing and regulating other immune cells destroying pathogens.

In conclusion, our findings demonstrated that there is a population of $\gamma\delta TCR^{+}CD11b^{+}$cells of *Plasmodium yoelii*-infected C57BL/6 mice spleen and contribute to *Plasmodium yoelii*-infection, which

might provide basic scientific knowledge for the development of new therapeutic approaches for the treatment of malaria patients.

Declarations

Ethics approval and consent to participate

6-8 weeks old female SPF C57BL/6 mice were purchased from the medical laboratory animal center of Guangzhou University of Chinese Medicine.

Competing interests

The authors declare that they have no competing interests.

Funding

This research was supported by grants from the Natural Science Foundation of Guangdong province (2020A1515010251, 2021A1515011032), Guangzhou science and technology project (202002030082), and the Open Foundation Key Laboratory of Tropical Diseases Control (Sun Yat-sen University), Ministry of Education (2021kfkt03).

Availability of data and materials

The datasets used and/or analysed during the current study are available from

the corresponding author on reasonable request.

Author contribution

XW, and JH conceived the study.DC, FM and ML performed the in vitro cellular test. FS and JX analysed the results. AX, LL and HX prepared parasite and animal. XP and JH contributed to the writing of the paper. All authors read and approved the final manuscript.

Acknowledgements

Not applicable.

References

1. *Wykes MN*, *Horne-Debets JM*, *Leow CY*, *Karunarathne DS*. *Malaria drives T cells to exhaustion*. *Front Microbiol 2014*; *5*: *249*.
2. *Wei H*, *Jin C*, *Peng A*, *Xie H*, *Xie S*, *Feng Y, et al. Characterization of γδT cells in lung of Plasmodium yoelii-infected C57BL/6 mice*. *Malar J 2021*; *20*: *89*.

3. *Tinto H, Otieno W, Gesase S, Sorgho H, Otieno L, Liheluka E, et al. Long-term incidence of severe malaria following RTS,S/AS01 vaccination in children and infants in Africa: an open-label 3-year extension study of a phase 3 randomised controlled trial. Lancet Infect Dis 2019; 19: 821 – 32.*
4. *Stiepel RT, Batty CJ, MacRaild CA, Norton RS, Bachelder E, Ainslie KM. Merozoite surface protein 2 adsorbed onto acetalated dextran microparticles for malaria vaccination. Int J Pharm 2021; 593: 120168.*
5. *Ramiro RS, Reece SE, Obbard DJ. Molecular evolution and phylogenetics of rodent malaria parasites. BMC Evol Biol 2012; 12: 219.*
6. *Xie H, Xie S, Wang M, Wei H, Huang H, Xie A, et al. Properties and Roles of γδT Cells in Plasmodium yoelii nigeriensis NSM Infected C57BL/6 Mice. Front Cell Infect Microbiol 2021; 11: 788546.*
7. *Maizels RM, Hewitson JP. Myeloid Cell Phenotypes in Susceptibility and Resistance to Helminth Parasite Infections. Microbiol Spectr 2016; 4.*
8. *Gabrilovich DI, Ostrand-Rosenberg S, Bronte V. Coordinated regulation of myeloid cells by tumours. Nat Rev Immunol 2012; 12: 253 – 68.*
9. *Hou N, Jiang N, Zou Y, Piao X, Liu S, Li S, et al. Down-Regulation of Tim-3 in Monocytes and Macrophages in Plasmodium Infection and Its Association with Parasite Clearance. Front Microbiol 2017; 8: 1431.*
10. *Chua CL, Brown G, Hamilton JA, Rogerson S, Boeuf P. Monocytes and macrophages in malaria: protection or pathology. Trends Parasitol 2013; 29: 26–34.*
11. *Woodberry T, Minigo G, Piera KA, Amante FH, Pinzon-Charry A, Good MF, et al. Low-level Plasmodium falciparum blood-stage infection causes dendritic cell apoptosis and dysfunction in healthy volunteers. J Infect Dis 2012; 206: 333 – 40.*
12. *Wykes MN, Good MF. What really happens to dendritic cells during malaria. Nat Rev Microbiol 2008; 6: 864 – 70.*
13. *Beetz S, Wesch D, Marischen L, Welte S, Oberg HH, Kabelitz D. Innate immune functions of human gammadelta T cells. Immunobiology 2008; 213: 173 – 82.*
14. *Xie H, Chen D, Li L, Yu X, Wu C, Gu H, et al. Immune response of γδT cells in Schistosome japonicum-infected C57BL/6 mouse liver. Parasite Immunol 2014; 36: 658 – 67.*
15. *Mamedov MR, Scholzen A, Nair RV, Cumnock K, Kenkel JA, Oliveira J, et al. A Macrophage Colony-Stimulating-Factor-Producing γδ T Cell Subset Prevents Malarial Parasitemic Recurrence. Immunity 2018; 48: 350 – 63.e7.*
16. *Legrand F, Driss V, Woerly G, Loiseau S, Hermann E, Fournié JJ, et al. A functional gammadeltaTCR/CD3 complex distinct from gammadeltaT cells is expressed by human eosinophils. PLoS One 2009; 4: e5926.*
17. *Sponaas AM, Freitas do Rosario AP, Voisine C, Mastelic B, Thompson J, Koernig S, et al. Migrating monocytes recruited to the spleen play an important role in control of blood stage malaria. Blood 2009; 114: 5522-31.*

18. *Patel SN, Serghides L, Smith TG, Febbraio M, Silverstein RL, Kurtz TW, et al. CD36 mediates the phagocytosis of Plasmodium falciparum-infected erythrocytes by rodent macrophages. J Infect Dis 2004; 189: 204 – 13.*
19. *Huang X, Huang S, Ong LC, Lim JC, Hurst RJ, Mushunje AT, et al. Differential Spleen Remodeling Associated with Different Levels of Parasite Virulence Controls Disease Outcome in Malaria Parasite Infections. mSphere 2016; 1.*
20. *Ghosn EE, Yang Y, Tung J, Herzenberg LA, Herzenberg LA. CD11b expression distinguishes sequential stages of peritoneal B-1 development. Proc Natl Acad Sci U S A 2008; 105: 5195 – 200.*
21. *Park KS, Park JH, Song YW. Inhibitory NKG2A and activating NKG2D and NKG2C natural killer cell receptor genes: susceptibility for rheumatoid arthritis. Tissue Antigens 2008; 72: 342-6.*
22. *Kumarasingha R, Ioannidis LJ, Abeysekera W, Studniberg S, Wijesurendra D, Mazhari R, et al. Transcriptional Memory-Like Imprints and Enhanced Functional Activity in γδ T Cells Following Resolution of Malaria Infection. Front Immunol 2020; 11: 582358.*
23. *Rowshanravan B, Halliday N, Sansom DM. CTLA-4: a moving target in immunotherapy. Blood 2018; 131: 58–67.*
24. *King T, Lamb T. Interferon-γ: The Jekyll and Hyde of Malaria. PLoS Pathog 2015; 11: e1005118.*
25. *Saraiva M, O'Garra A. The regulation of IL-10 production by immune cells. Nat Rev Immunol 2010; 10: 170 – 81.*
26. *Lewis MD, Langhorne J. A New Link between γδ T Cells and Myeloid Cells in Malaria. Immunity 2018; 48: 193-5.*
27. *Han B, He Y, Zhang L, Ding Y, Lian L, Zhao C, et al. Long intergenic non-coding RNA GALMD3 in chicken Marek's disease. Sci Rep 2017; 7: 10294.*
28. *Gao SP, Sun HF, Jiang HL, Li LD, Hu X, Xu XE, et al. Loss of COX5B inhibits proliferation and promotes senescence via mitochondrial dysfunction in breast cancer. Oncotarget 2015; 6: 43363-74.*
29. *Hu T, Xi J. Identification of COX5B as a novel biomarker in high-grade glioma patients. Onco Targets Ther 2017; 10: 5463-70.*
30. *Rose S, Misharin A, Perlman H. A novel Ly6C/Ly6G-based strategy to analyze the mouse splenic myeloid compartment. Cytometry A 2012; 81: 343 – 50.*
31. *Saiwai H, Kumamaru H, Ohkawa Y, Kubota K, Kobayakawa K, Yamada H, et al. Ly6C + Ly6G- Myeloid-derived suppressor cells play a critical role in the resolution of acute inflammation and the subsequent tissue repair process after spinal cord injury. J Neurochem 2013; 125: 74–88.*
32. *Van Ginderachter JA, Beschin A, De Baetselier P, Raes G. Myeloid-derived suppressor cells in parasitic infections. Eur J Immunol 2010; 40: 2976-85.*

Figures

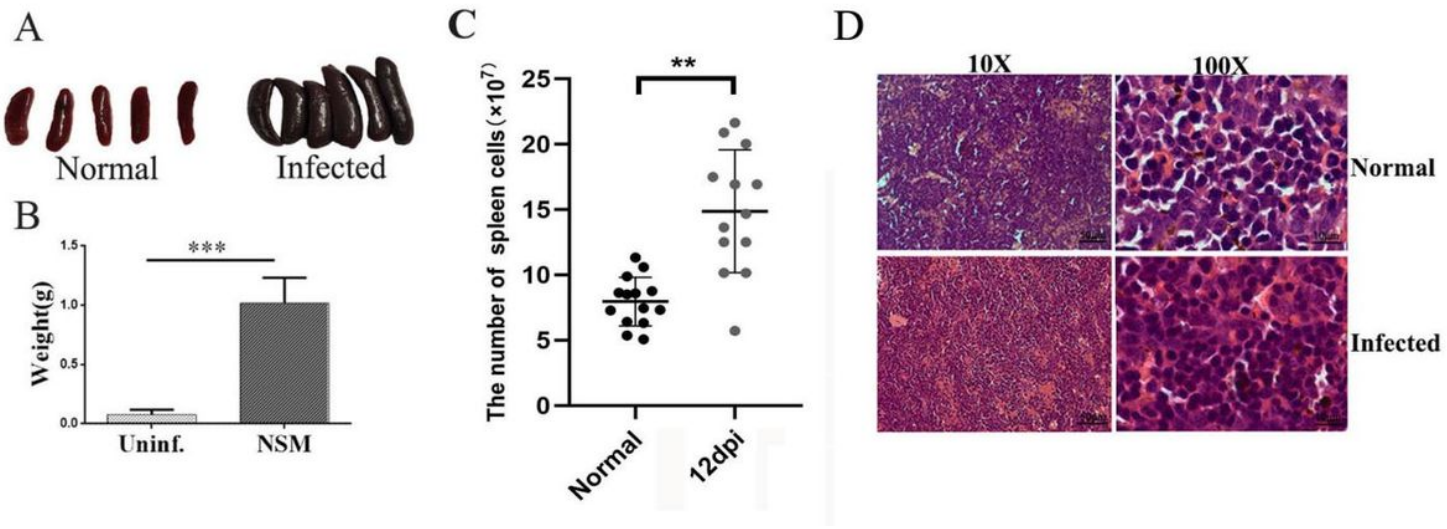

Figure 1

Splenic lesions in mice infected with *Plasmodium*. (A) Comparison of the spleen appearance in normal and infected mice. Representative samples were shown for each group. (B and C) Comparison of the weight of the spleen and numbers

of extracted spleen cells from normal or infected mice. (D) HE staining of the spleen tissue. $^{**}P<0.01$,$^{*}P<0.001$.

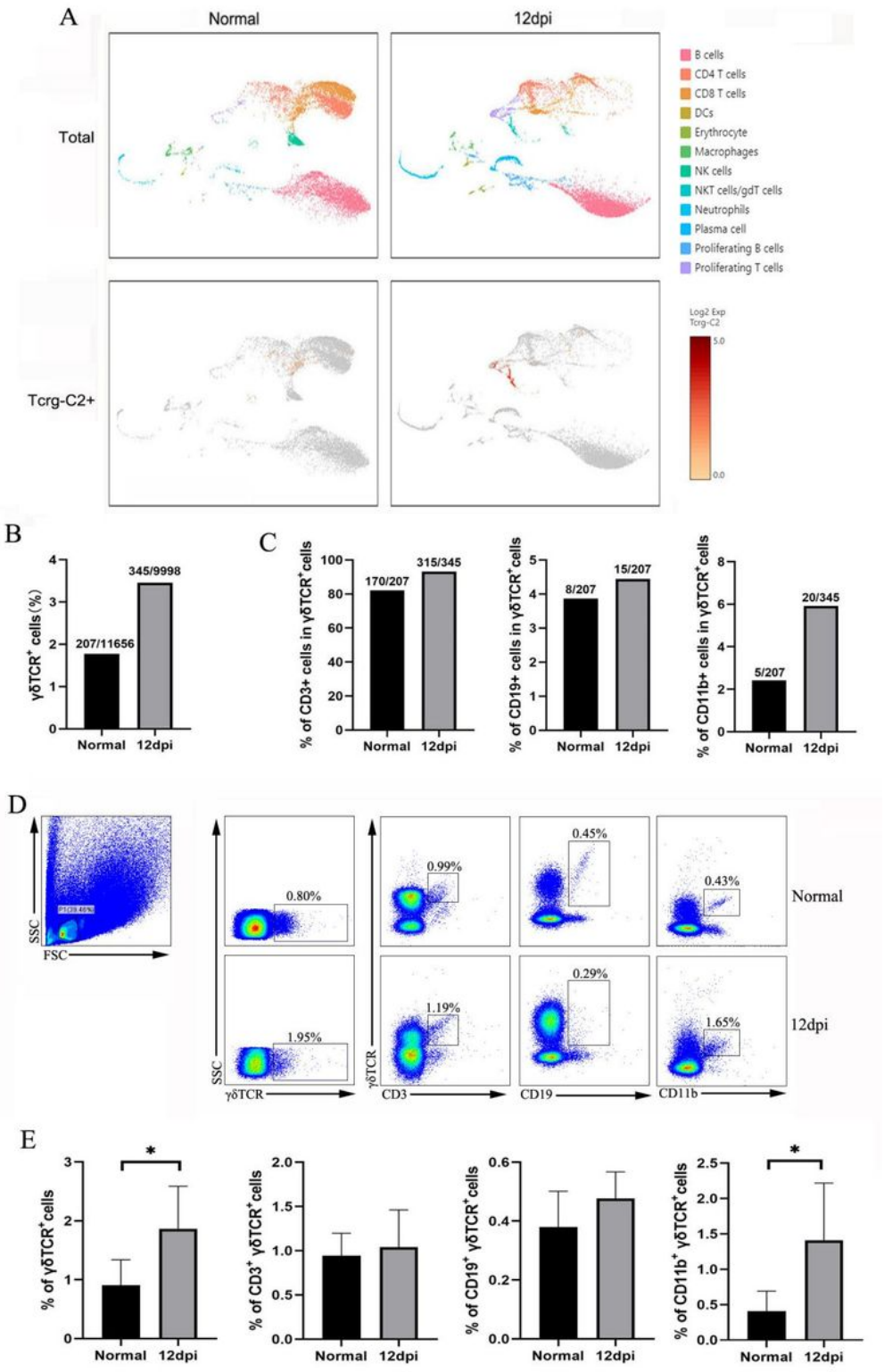

Figure 2

The expression of γδTCR$^+$ cells. (A) UMAP feature plots showing expression of *Tcrg-C2* gene based on control vs. 12dpi cells. Feature expression represented by color gradient, with high expression represented by red and low expression represented by gray. (B) Comparison of the proportion of γδTCR$^+$ cells in the whole cells from normal or infected mice. (C) The proportions of CD3$^+$ cells, CD19$^+$ cells and CD11b$^+$ cells

to γδTCR$^+$ cells in normal and infected mice were analysed. (D) Splenocytes were separated from naive and infected mice (12days post infection) and then stained with monoclonal antibodies against mouse γδTCR, CD3, CD19 and CD11b after cell surface staining. The representative dot plots were shown. (E) Results represent mean percentages (SD) of γδTCR$^+$cells, γδTCR$^+$CD3$^+$ cells, γδTCR$^+$ CD19$^+$cells andγδTCR$^+$ CD11b$^+$cells from normal and infected spleen.

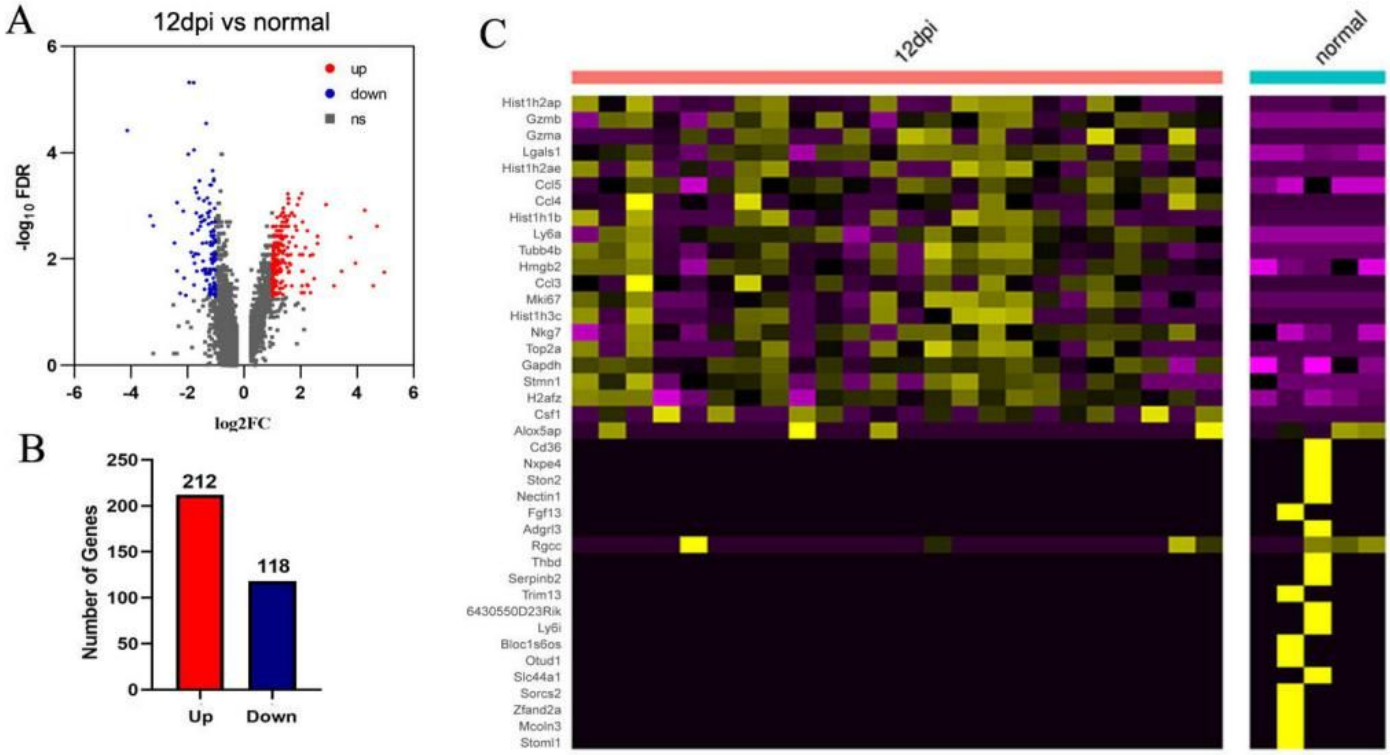

Figure 3

The differentially expressed genes (DEGs) analysis. (A) Volcano plot displaying the DEGs in 12dpi vs. normal cells. The up-regulated genes (red), and down-regulated (blue) genes are indicated. Gray dots represent non-DEGs (<1.5-fold change). (B) The number of up-regulated and down-regulated genes was shown.(C) Gene expression heatmap of 40 top DEGs.

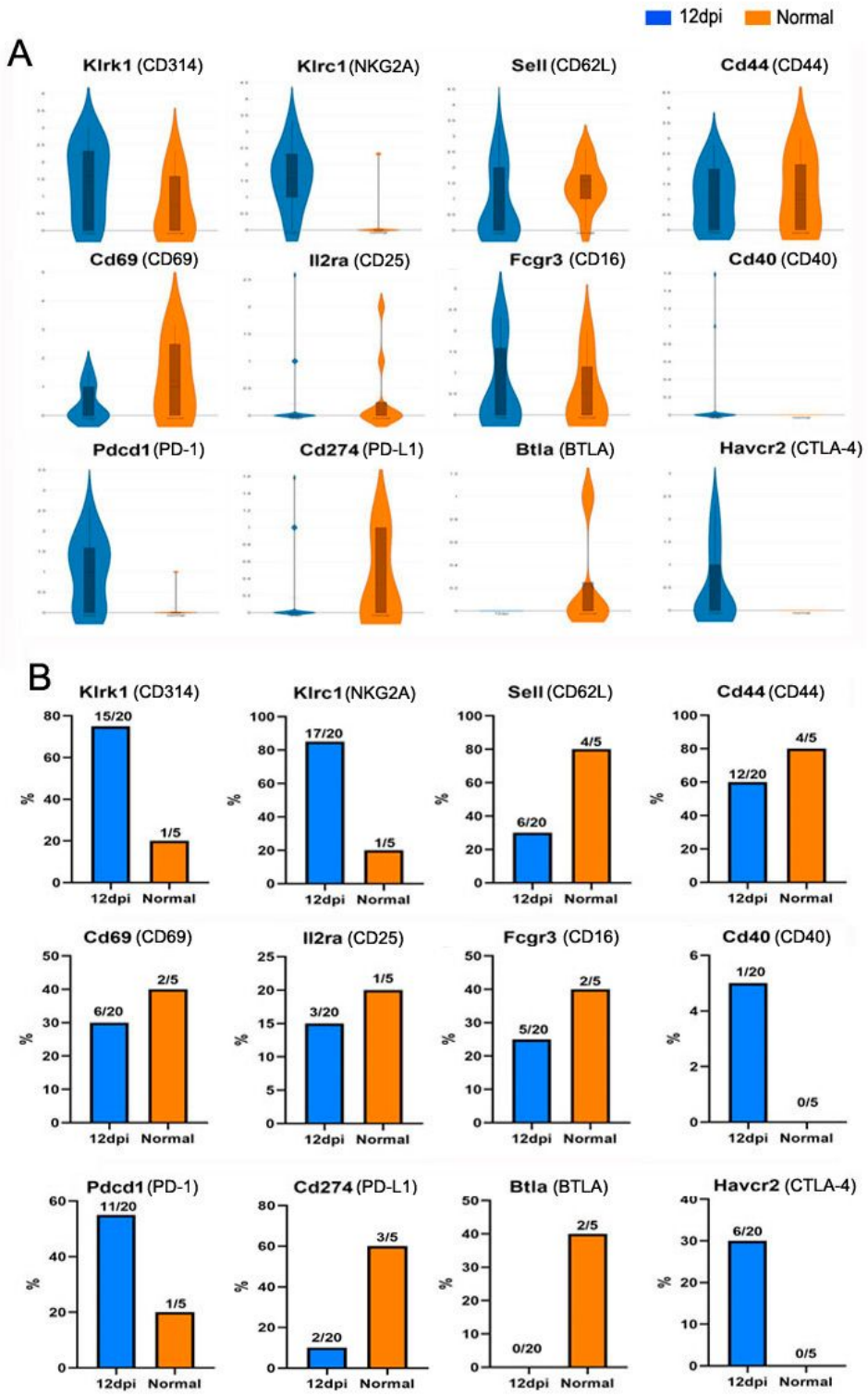

Figure 4

The analysis of state related genes. (A) Violin plot displaying the expression of representative state related genes in γδTCR^{+}CD11b^{+} cell, and orange, blue represent the categories of 12dpi and normal, respectively. (B) The proportion of cells that expressed those genes within the whole γδTCR^{+}CD11b^{+} population.

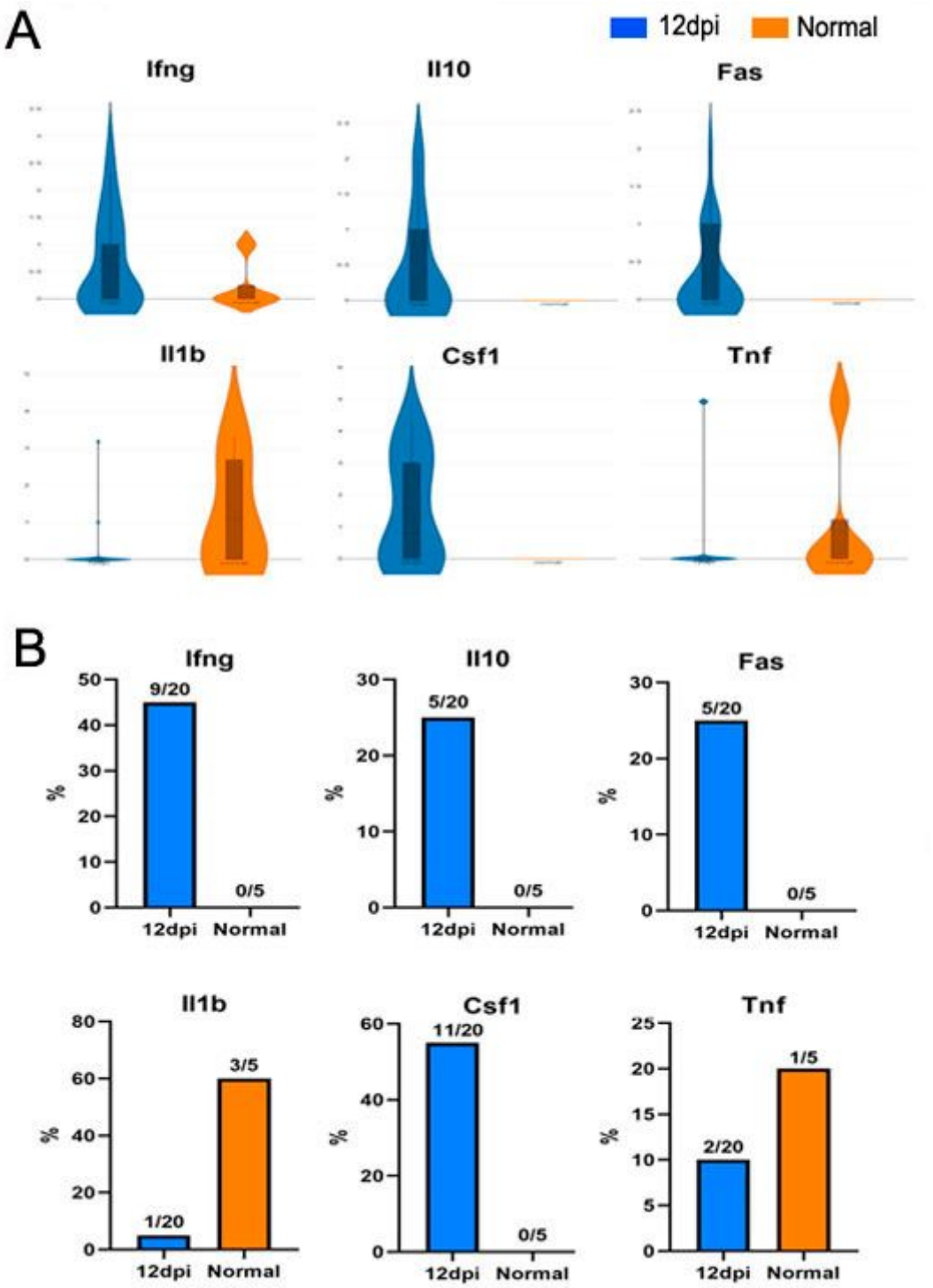

Figure 5

The analysis of cytokine related genes. (A) Violin plot show expression level of representative cytokines related genes expressed in γδTCR^{+}CD11b^{+} cell. (B) The proportion of cells that expressed those genes within the whole γδTCR^{+}CD11b^{+} population.

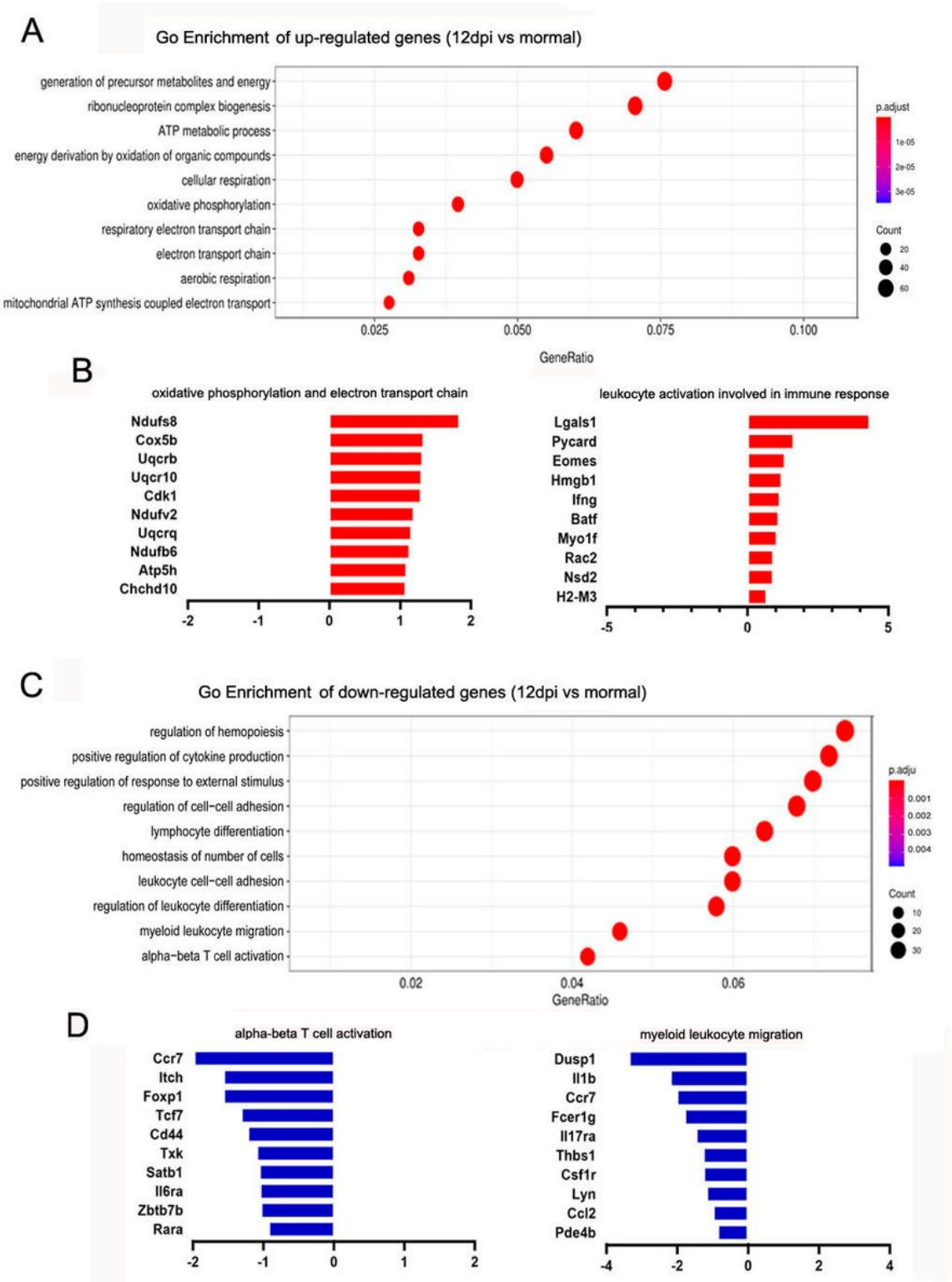

Figure 6

GO enrichment of different expressed genes. (A and C) GO enrichment of top ten up- expressed (A) or downregulated (C) genes in 12dpi vs. control cells.

(B and D) Log fold change of individual genes in selected pathways upregulated (B) or downregulated (D) in 12dpi vs. control cells.

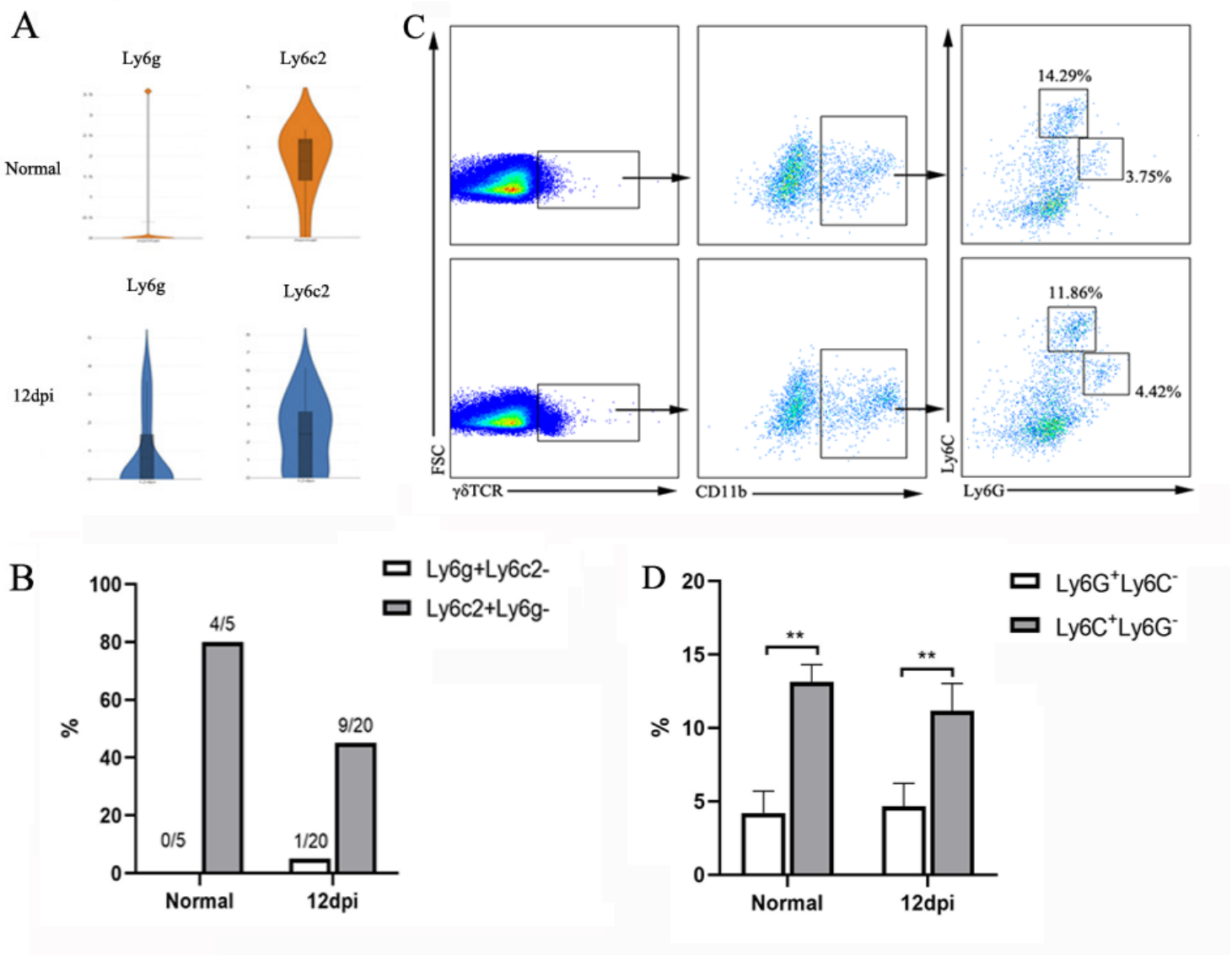

Figure 7

The phenotypes of γδTCR$^+$CD11b$^+$ cell cells subsets

(A) Violin plot displaying the expression of Ly6g and Ly6c2 genes in γδTCR$^+$CD11b$^+$ cell, and orange, blue represent the categories of 12dpi and normal, respectively. (B) The proportion of cells that expressed those genes within the whole γδTCR$^+$CD11b$^+$ population. (C) The dot plots show staining with PerCP-cy5.5-conjugated anti-Ly6C mAbs and PE-conjugated anti-Ly6G mAbs of γδTCR$^+$ CD11b$^+$cells by FACS analysis. The representative dot plots were shown. (D) Results represent mean percentages (SD) of Ly6G$^+$Ly6C$^-$cells and Ly6C$^+$Ly6G$^-$from normal and infected spleen.